JOURNAL OF COMPUTATIONAL PHYSICS **48**, 284–301 (1982)

Three-Dimensional Boundary Conditions in Supersonic Flow

S. RUDMAN AND F. MARCONI

Grumman Aerospace Corporation Research and Development Center, Bethpage, New York 11714

Received January 7, 1982

A theoretical analysis of the flow pattern at a solid surface in three-dimensional supersonic flow is presented. The purpose of the study is to develop the additional information necessary to overcome the nonuniqueness associated with the body tangency condition in three dimensions. The analysis is based on the fact that three-dimensional waves propagate locally exactly as they do in axisymmetric flow when viewed in the osculating plane to streamline. The supersonic flow over an infinite swept corner is examined by both the classical solution and the three-dimensional solution in the osculating plane; the results are shown to be identical. A simple numerical algorithm is proposed which accounts for the three wave surfaces that interact at a solid boundary.

INTRODUCTION

Future success in the prediction of complex three-dimensional supersonic flow fields will require increased theoretical understanding of such phenomena. In particular, the key to accurate and reliable numerical computations lies in the proper imposition of boundary conditions. A variety of three-dimensional boundary point algorithms have been developed which are based on method of characteristic type analysis of the governing equations. The techniques reported in [1–5] rely on the reduction of the full equations to a reference plane system in two space dimensions. The reference plane is employed in the vicinity of the boundary point in which the calculation is performed. The orientation of this plane relative to the boundary surface has been chosen, in the past, based on intuitive and ad hoc reasoning. Velocity components and gradients normal to the reference plane appear as forcing terms in the characteristic equations. Theoretical analysis of the full three-dimensional Euler equations [6] indicates that there is a unique plane in which the flow is equivalent to an axisymmetric (a two space dimension) flow. There is no velocity component normal to this plane and the only term appearing in the equations beyond pure planar two-dimensional expressions is a velocity gradient term analogous to that appearing in the axisymmetric equations. It is the object of this paper to study the implications of employing these concepts in the boundary point calculations involved in three-dimensional supersonic flows.

The complexities of three-dimensional flow calculations as compared to their two-dimensional counterparts are manifest in the application of the boundary conditions. In two-dimensional supersonic flow there is a well-developed theoretical basis [7–9]

0021-9991/82/110284–18$02.00/0

upon which to model the numerical simulation of the boundary surface/flow interactions. Moretti [10, 11] was the first to recognize that the standard finite difference algorithms employed for interior point calculations had to be replaced by a local solution based on the method of characteristics at solid boundary points as well as at shock points. Later, Abbett [5] showed how to combine finite difference calculations with a local Prandtl–Meyer solution at a solid boundary and thus greatly reduce the complexity of the boundary point calculation. DeNeff [12] and Rudman [13] extended this method to shock surface and contact surface boundary point calculations. The central new feature that arises in the three-dimensional calculation is the nonunique nature of the boundary conditions. At a solid surface, for example, the boundary condition that the velocity vector be tangent to the surface is a single condition for the two unknown cross flow angles. In two dimensions a single flow angularity unambiguously determines the ratio of the two velocity components. In three dimensions the surface tangency condition determines only a single linear relationship between the two cross flow velocities. The resolution of this ambiguity is addressed.

The class of boundary point algorithm under consideration employs first a finite difference calculation and then a "correction" to satisfy the surface tangency requirement. That is, the flow properties at the unknown point are computed using a variation of the finite difference scheme at the interior points. A modified interior point calculation is necessary because no mesh points are computed interior to the body. Either one-sided differences away from the body are employed to model the normal derivatives or a reflection plane is used to define hypothetical flow properties at a surface one mesh width interior to the body. The flow properties so computed at the unknown point (Fig. 1) do not in general satisfy the body tangency condition and

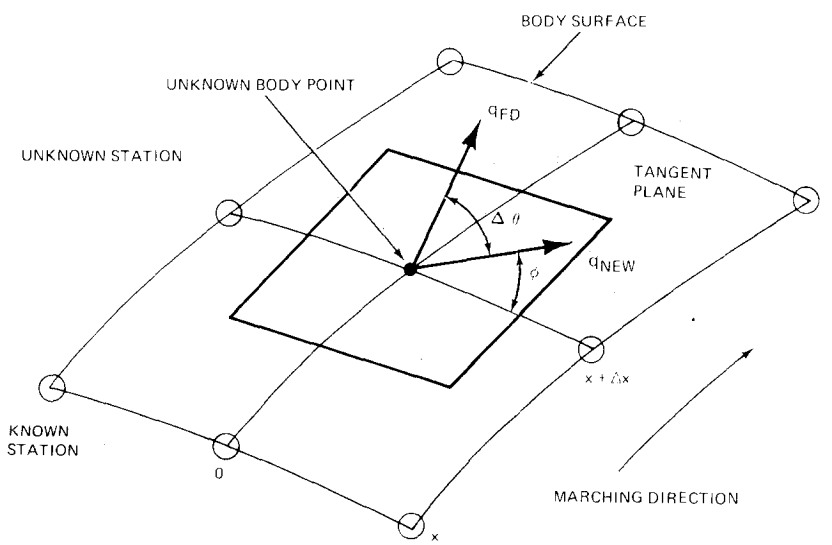

FIG. 1. Schematic of the computational mesh at a solid boundary point.

are denoted FD (finite difference). Following the methods of [5, 8, 9] a wave is added to the solution at the boundary point (the correction) to bring the velocity in line with the desired direction. In two-dimensional flow this is a simple Prandtl–Meyer wave. In three-dimensional flow the orientation of the "correction" wave is not known a priori. Any rotation into the tangency plane satisfies the boundary condition. In the notation used in Fig. 1 the value of ϕ is unknown and must be determined from a detailed analysis of the flow.

The first step in developing the required information is recognizing that three-dimensional supersonic flow is locally directly analogous to a two space dimension (axisymmetric) flow [6] when viewed in the osculating plane to the streamline. In supersonic flow all changes in flow properties are brought about by wave surfaces. Each wave surface in three-dimensional flow when viewed locally is a plane wave moving at the local speed of sound relative to the fluid. The component of velocity normal to the wave front is sonic. Beyond that the orientation for the wave front is arbitrary so that it can rotate the oncoming velocity both vertically and horizontally depending on its strength and direction. In two-dimensional flow, by contrast, the waves rotate the flow either upward or downward (first or second family waves) about an axis perpendicular to the plane of motion. In three-dimensional flow the rotation takes place about the binormal vector to the local streamline direction. The direction of the local binormal vector is determined by the wave orientation.

In the following sections further discussion of the role of the osculating plane in three-dimensional flow will be presented. These concepts identify two main bicharacteristics in the fore Mach cone (the intersection of the cone and the osculating plane) that determine the solution at any point. This description of the flow is then reconciled with the classical solution for flow over an infinite swept expansion (or compression) corner which is the prototype model for plane wave solutions. It is shown that the classical solution which is achieved by examining the flow in a plane normal to the sweep line is identical with the solution employing the osculating plane. For infinitesimal rotations the flow over the corner is a Prandtl–Meyer expansion (compression) for the total velocity vector. The rotation is about the binormal vector defined by $\nabla p \times \mathbf{q}$. At the body surface three wave fronts determine the solution: an incident wave, a reflected wave, and a wave emitted by the body. In general, the sweep angle of the incident/reflected waves has a binormal vector associated with it. In the context of numerical calculations these waves are considered infinitesimal, i.e., the body slope and the flow properties change in proportion to the step size. Because infinitesimal rotations can be added, the rotations of each wave can be combined to yield a single binormal vector which defines the interaction at the body surface. A three-dimensional boundary point calculation procedure is set forth based on these ideas. In the procedure the incident wave and reflected waves are computed as part of the finite difference calculation, substantially simplifying the algorithm. The final rotation (correction) about the binormal vector associated with the change in body slope accounts for the emitted wave.

THREE-DIMENSIONAL WAVES

A streamline in three-dimensional space has the general properties of any line in space. Figure 2 shows the unit vector triad defined by the tangent, normal, and binormal vectors at point 0. At 0 the velocity vector is parallel to the tangent vector. The streamline has a principal curvature in the normal direction. The acceleration of the fluid element at point 0 is in the $t-n$ plane and the streamline remains in the $t-n$ plane to second order. The streamline has a torsion in the binormal direction but this results in a higher-order displacement. The Euler equations written using as local Cartesian coordinates t, n, b with velocity components, U, V, W are [6]

$$(\rho U)_t + (\rho V)_n + \rho W_b = 0, \tag{1}$$

$$\rho U U_t + \rho V U_n + p_t = 0, \tag{2}$$

$$\rho U V_t + \rho V V_n + p_n = 0, \tag{3}$$

$$p_b = 0, \tag{4}$$

$$\tfrac{1}{2}(U^2 + V^2) + \gamma p/(\gamma - 1)\rho = h_0. \tag{5}$$

The fact that $W = 0$ at point 0 has been employed throughout. The momentum equation in the b direction (Eq. (4)) expresses mathematically the fact that there are no accelerations (or forces) in the b direction. Equations (1)–(3) and (5) are the familiar Euler equations in two space dimensions with the single additional term ρW_b

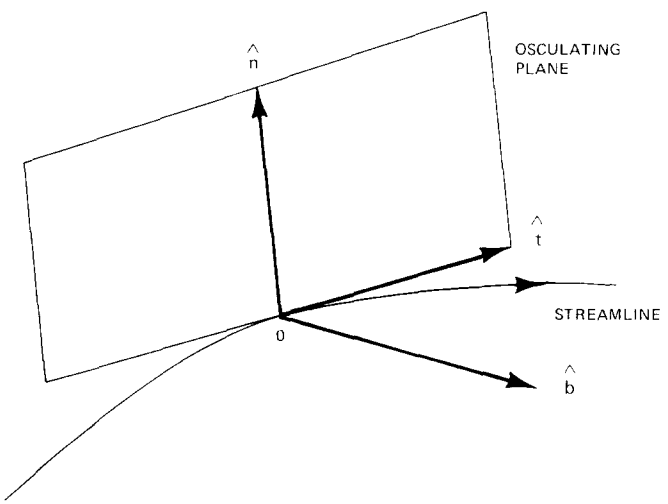

FIG. 2. The osculating plane to a streamline.

in the continuity equation. This term is analogous to the forcing term in axisymmetric flow and produces intensification or decay as the wave progresses. Based on our understanding of axisymmetric flow, this term does not produce qualitative changes in the wave nature of the solution.

The local solution to the flow is defined by a two space dimension problem exactly like axisymmetric flow. Figure 3 is a schematic of the wave pattern near point 0. The intersection of the Mach cone through 0 and the osculating $(t-n)$ plane are two bicharacteristics. These two lines carry the same characteristic information as first and second family waves in axisymmetric flow. The full three-dimensional equations defined the Mach cones as possible characteristic surfaces as an expression of the fact that wave fronts can propagate at any arbitrary orientation to the local velocity vector. The local analysis presented in [6] and sketched out here shows that when the flow is not singular at point 0 only two bicharacteristics are at work. These bicharacteristics are in the osculating plane containing ∇p, the only force on the fluid element.

In order to develop further confidence in these ideas and get quantitative results, we examine the model problem of an infinite swept expansion using the classical solution and then the osculating plane analysis. The solution is examine at the point where the deflection occurs so that no wave intensification or decay is considered. Figure 4 is a sketch of the flow which is infinite in the y or chord direction. A uniform flow parallel to a flat surface expands about a corner (true angle normal to the sweep line δ) which is swept relative to the oncoming velocity vector by the angle Λ. In the classical solution the oncoming velocity vector is decomposed into components normal and tangential to the sweep line. The tangential velocity vector is

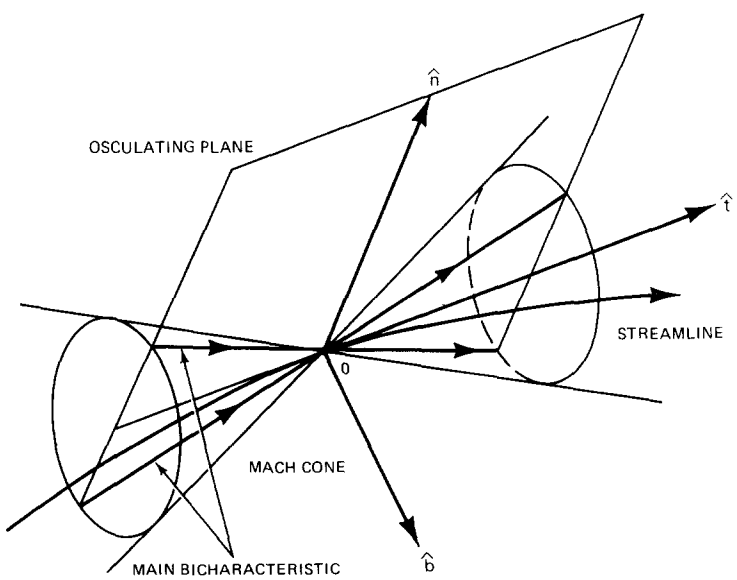

FIG. 3. The Mach cone and the main bicharacteristics.

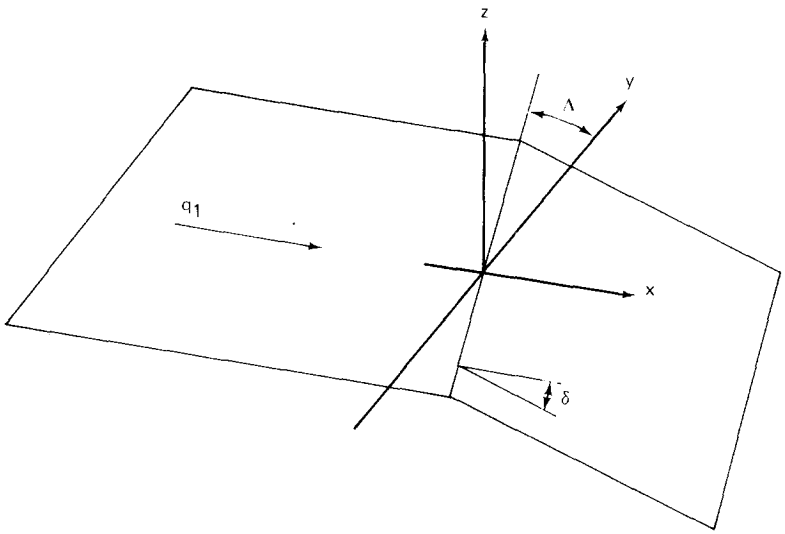

FIG. 4. Schematic of the geometry for the infinite swept expansion corner.

unchanged by the corner while the normal component undergoes a two-dimensional expansion through the angle δ. Denoting downstream conditions by 2 and oncoming conditions by 1,

$$\mathbf{q}_1 = q_{1n}\hat{N}_1 + q_{1t}\hat{T}, \tag{6}$$

$$\mathbf{q}_2 = q_{2n}\hat{N}_2 + q_{2t}\hat{T}, \tag{7}$$

where $\hat{N}$ is the unit vector normal to the sweep line lying on the surface and $\hat{T}$ is the unit vector tangent to the sweep line. Furthermore,

$$q_{2n} - q_{1n} = q_{1n}\delta/\sqrt{M_n^2 - 1} = q_{1n}\delta \tan \mu_n, \tag{8}$$

$$q_{2t} = q_{1t}, \tag{9}$$

$$M_n = M_1 \cos \Lambda, \tag{10}$$

where Eq. (8) is the Prandtl–Meyer relationship for an infinitesimal wave which turns a flow at Mach number M_n an angle δ. Combining (8) and (9) with (7), using

$$\hat{N}_2 = (\cos \Lambda \cos \delta, \sin \Lambda, \cos \delta - \sin \delta), \qquad \hat{T} = (\sin \Lambda, -\cos \Lambda, 0),$$

and retaining only first-order terms,

$$\mathbf{q}_2 = q_1(1 + \delta \cos^2 \Lambda \tan \mu_n, \delta \sin \Lambda \cos \Lambda \tan \mu_n, -\delta \cos \Lambda), \tag{11}$$

where q_1 is the magnitude of the upstream velocity.

The change in the magnitude of the velocity vector is given by

$$\frac{\Delta q}{q_1} = \frac{q_2 - q_1}{q_1} = \sqrt{(1 + \delta \cos^2 \Lambda \tan \mu_n)^2 + (\delta \sin \Lambda \cos \Lambda \tan \mu_n)^2 + \delta^2 \cos^2 \Lambda} - 1;$$

retaining only the highest order terms

$$\Delta q/q_1 = \delta \cos^2 \Lambda \tan \mu_n. \tag{12}$$

A sketch of the wave pattern is shown in Fig. 5. A plane wave is emitted by the sweep line at a true angle μ_n given by the expression

$$\sin \mu_n = 1/M_n = 1/M_1 \cos\Lambda = \sin \mu_1/\cos \Lambda.$$

The flow is turned by this wave front about a vector

$$\mathbf{R} = \mathbf{q}_1 \times \mathbf{q}_2/q_1^2 = (0, \delta \cos \Lambda, \delta \sin \Lambda \cos \Lambda \tan \mu_n). \tag{13}$$

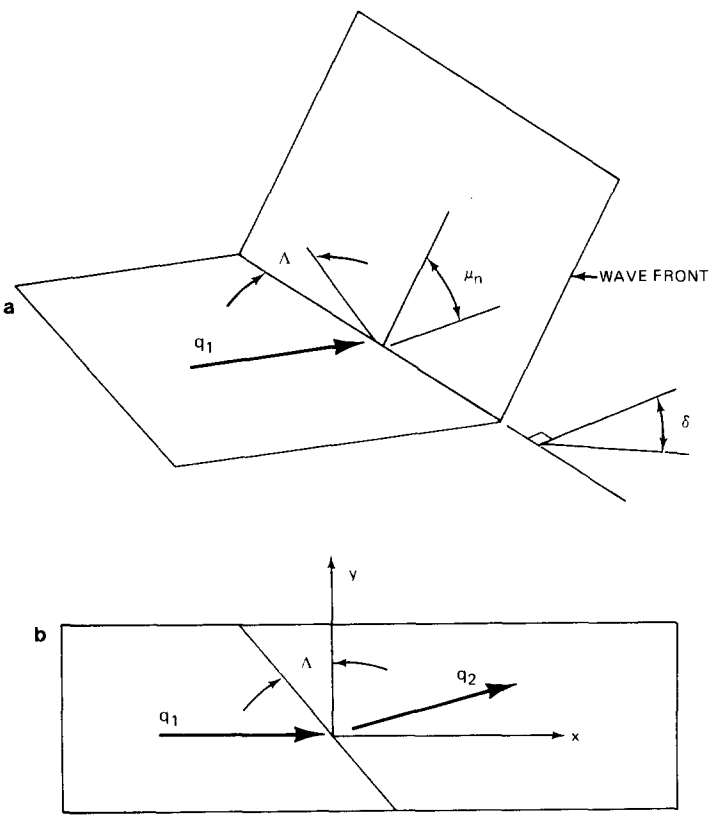

FIG. 5. Wave pattern at swept leading edge. (a) Wave front plane. (b) Top view.

It is interesting to note that the rotation line is not parallel to the sweep line; in fact, it has no x component. It is inclined to the $x-y$ plane by the angle β

$$\tan\beta = \cot\mu_n \sin\Lambda. \tag{14}$$

The direction of the initial and final velocity vectors can be related by a simple rotation about the vector **R**. The angle between these two directions in the plane normal to **R** is (see Appendix)

$$\delta' = \delta \cos\Lambda \cos\mu_1/\cos\mu_n = \delta \cos^2\Lambda \cos\mu_1/\sqrt{\cos^2\Lambda - \sin^2\mu_1}. \tag{15}$$

In the following paragraphs it will be shown that this exact solution can be achieved by solving the three-dimensional flow problem using the osculating plane. The bicharacteristic in the osculating plane is first located as the line of tangency of the wave front leaving the swept leading edge and the Mach cone. The osculating plane is then shown to be perpendicular to the rotation vector **R** from the classical solution. The $\vec{\delta}$ vector and the **R** vector are parallel and the required deflection is exactly that given by Eq. (15). Then it is shown that the final velocity achieved by expanding (or compressing) the total velocity q_1 through the rotation δ' results in the same magnitude of the final velocity as the classical solution. Thus since the rotation direction, magnitude of rotation, and final velocities are identical, the two solutions are identical.

Referring to Fig. 6, at any point on the sweep line a Mach cone is emitted with half angle $\mu_1 = \sin^{-1}(1/M_1)$. The Mach cone at the origin is shown on the figure but all others are similar. The wave front attached to the sweep line rests on the Mach cones. The intersection (tangency line) of this wave front and the Mach cone occurs along a line (bicharacteristic) which can be easily found geometrically using vector analysis (see Appendix). In the cross-sectional view (Fig. 6b) the angle ξ locating this line is given by

$$\cos\xi = \tan\mu_1 \tan\Lambda. \tag{16}$$

The tangent of this angle can be found by standard trigonometric relationships and related to μ_n (see Appendix)

$$\tan\xi = 1/\tan\mu_n \sin\Lambda. \tag{17}$$

A vector tangent to the plane containing the intersection line and the axis of the Mach cone (streamline direction) is therefore

$$\mathbf{T} = (0, -1, \tan\xi).$$

A vector parallel to the rotation vector **R** (Eq. (13)) is

$$\mathbf{R}_1 = (0, 1, \sin\Lambda \tan\mu_n).$$

The dot product of $\mathbf{R}_1$ and **T** is always zero.

$$\mathbf{T}\cdot\mathbf{R}_1 = -1 + \tan\xi \sin\Lambda \tan\mu_n = -1 + 1 = 0 \tag{18}$$

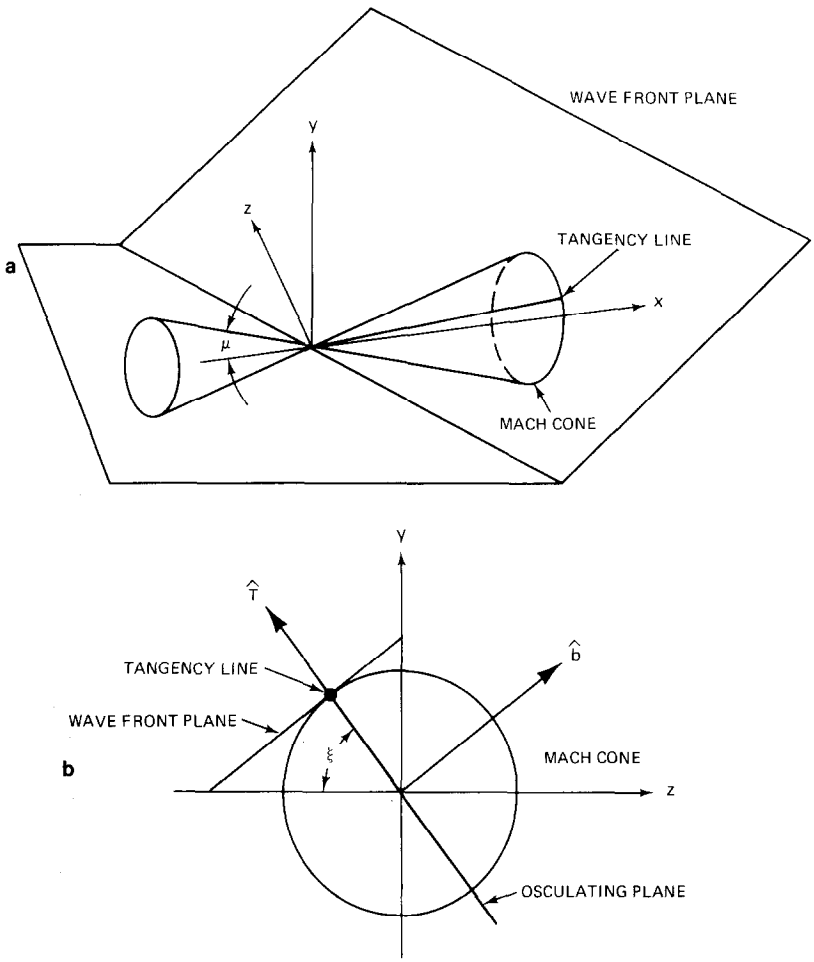

FIG. 6. The Mach cone, osculating plane, and wave front plane for the swept expansion. (a) Three-dimensional view. (b) Cross section in $y-z$ plane.

Therefore the $\hat{b}$ vector, which is normal to the osculating plane, and the **R** vector are parallel.

The $\hat{b}$ vector and **R** are parallel and the same turning angle δ' is specified by Eq. (15) in both solutions. All that remains is to show that expanding the total velocity q_1 an amount δ' changes its magnitude to the same value as the classical solution. The change in velocity is given by the Prandtl–Meyer expression. (This is the expression used in Eq. (8).)

$$\Delta q/q_1 = -\Delta\theta \tan \mu_1$$

In this case $\Delta\theta = -\delta'$, so $\Delta q/q_1 = \delta' \tan \mu_1$. Using the value of δ' given by Eq. (15),

$$\Delta q/q_1 = \delta \cos\Lambda \sin \mu_1 / \cos \mu_n ; \tag{19}$$

$M_n = M_1 \cos \Lambda$, therefore

$$\sin \mu_1 = \sin \mu_n / \cos \Lambda.$$

Substituting this in Eq. (19) yields

$$\Delta q/q_1 = \delta \cos^2 \Lambda \tan \mu_n \tag{20}$$

The results are identical to Eq. (12).

The conclusion is summarized in Fig. 7. The flow over the swept expansion (or compression) corner can be evaluated by using the bicharacteristics in the osculating plane. The orientation of the osculating plane is determined by the relative orientation of the sweep line and the oncoming velocity. In the osculating plane, Fig. 7b, the flow is two-dimensional and the incoming wave is oriented at the free stream Mach angle μ_1.

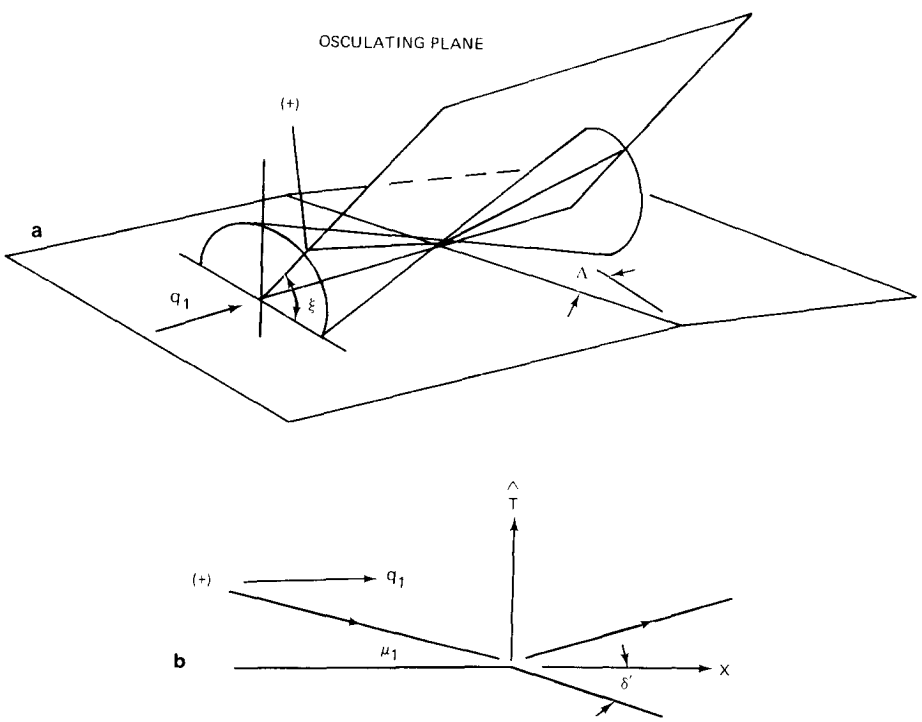

FIG. 7. Three-dimensional representation of swept expansion corner. (a) The main bicharacteristics for the swept corner. (b) Characteristics in the osculating plane.

The Boundary Conditions at a Solid Wall

The purpose of the previous discussion was to demonstrate that the wave processes in three-dimensional flow are in fact locally equivalent to the familiar two-dimensional wave process. The passing of an infinitesimal strength wave front in three-dimensional flow produces a change in flow direction, magnitude of velocity, and hence pressure and density given by the Prandtl–Meyer relationship. The orientation of the deflection is given by a rotation about the binormal vector whose direction is determined by the relative orientation of the oncoming velocity and the wave front. In general in a three-dimensional flow there can be an arbitrary number of wave fronts passing a given point. Each wave front has a given strength and associated binormal vector. Because the waves under discussion are infinitesimal in strength, the rotations they produce are additive as are the increments in velocity. Therefore at any given point the effect of all wave fronts can be added to produce one binormal vector associated with all the changes in the flow properties at that point.

The wave pattern at a solid surface is shown schematically in Fig. 8. In general there are three wave fronts that must be considered: an incident wave, its reflected wave, and an emitted wave. The incident wave originates in the flow and strikes the boundary. Upstream of this wave the flow is parallel to the surface. A reflected wave front originates at the body surface to bring the flow parallel to the surface. These two waves intersect the body along line *BB* in Fig. 8. In addition at point 0 the body

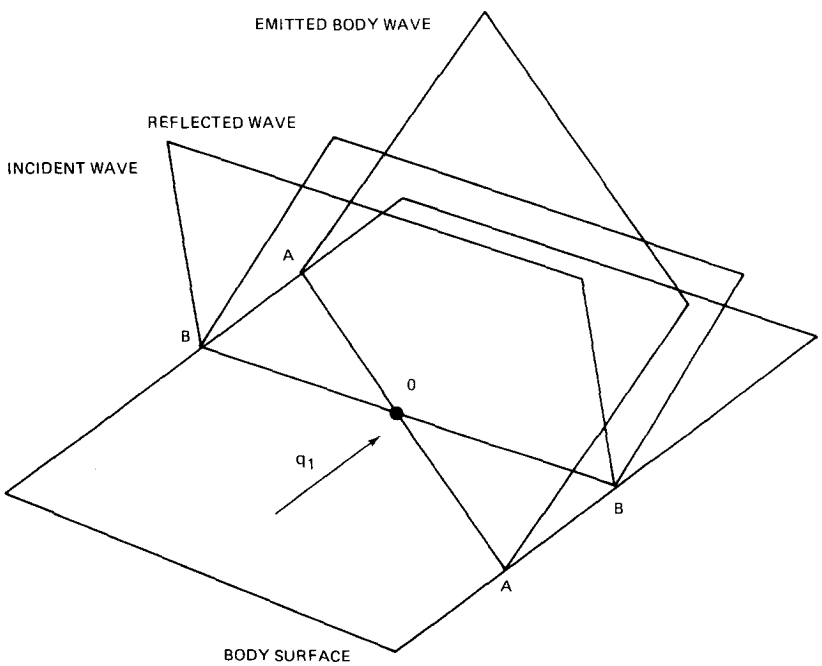

FIG. 8. Wave pattern at a solid surface.

surface may change orientation. This results in a wave front moving away from the surface which originates on the body along line AA. This wave front rotates the velocity vector to make it parallel to the new body direction. The lines AA and BB are swept at different angles to the oncoming flow. This is one reason that the three-dimensional boundary condition is more complex than the two-dimensional counterpart. In two-dimensional flow AA and BB are coincident as are the emitted and reflected waves. In that case there is no need to distinguish between the reflected wave and the emitted wave.

With this theoretical background it is now possible to suggest an algorithm for the correct imposition of the boundary condition at a solid surface in three-dimensional flow. Figure 9 shows a portion of the computational mesh. At station x all flow properties are known at the interior points and the boundary points. The boundary point denoted N at station $x + \Delta x$ is to be computed. Using a grid that is orthogonal to the body surface, an additional line of mesh points interior to the body is defined using reflection conditions (more discussion later on these values). The standard interior point calculation is performed at point 0 to compute values at N. The values so computed at point N account for the incident and reflected waves by virtue of the construction of the reflected points. The emitted wave is now added by expanding (or compressing) the flow to the new body slope. This can be achieved by either of the two methods discussed in the previous paragraphs. The sweep line of this expansion is determined by taking the cross product of the new body normal at N and the normal at 0 (Fig. 10).

The one question that remains is the specification of the flow properties on the reflection plane. The flow properties required on the reflection plane are computed by the usual formulas despite the fact that there is wave intensification due to the

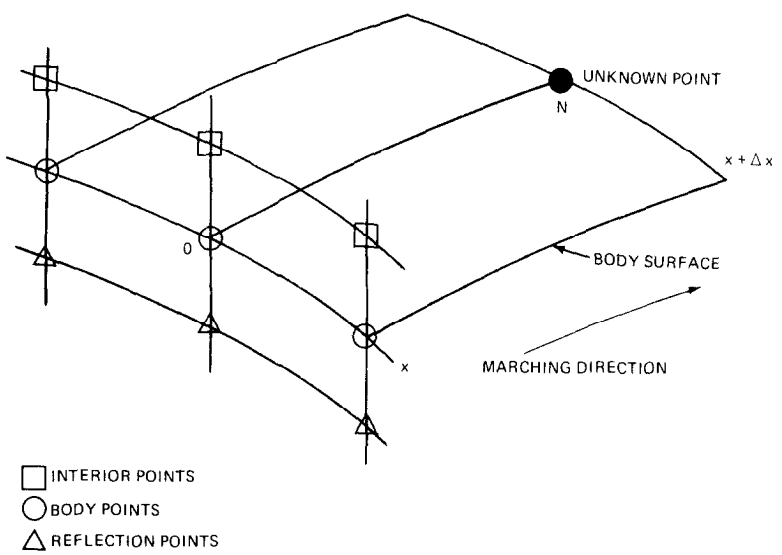

FIG. 9. Computational mesh for boundary point calculation.

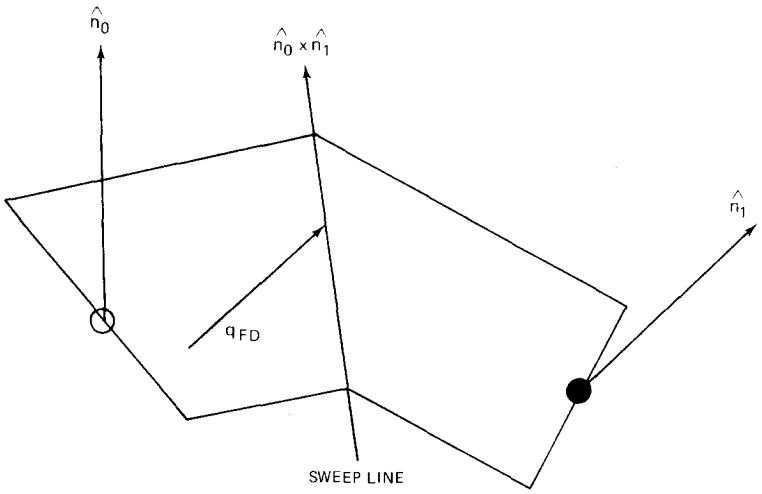

FIG. 10. Geometry for emitted body wave.

velocity gradient normal to the osculating plane. Scalar variables and velocity components parallel to the plate are reflected using symmetry conditions while the velocity component normal to the plane is reflected using antisymmetry. Figure 11a shows a schematic of the osculating plane at the boundary point N for the incident/reflected wave process. Figure 11b is the wave pattern in the osculating plane. The characteristic starting at B reaches the body surface at N and propagates into the flow as the reflected wave. In the osculating plane the wave propagation process is equivalent to an axisymmetric flow [6]. The characteristic equations governing axisymmetric waves are [7]:

$$dv + d\theta = K\,ds \qquad \text{along} \quad AN, \tag{21}$$

$$dv - d\theta = K\,ds \qquad \text{along} \quad BN, \tag{22}$$

where v is the Prandtl–Meyer function, s is distance along the characteristic, and K is the forcing term due to the velocity gradient normal to the characteristics.

These equations are integrated in the usual manner,

$$v_N - v_A + \theta_N - \theta_A = \tfrac{1}{2}(K_A + K_N)\, s_{AN} + O(s^3), \tag{23}$$

$$v_N - v_B - \theta_N + \theta_B = \tfrac{1}{2}(K_B + K_N)\, s_{BN} + O(s^3). \tag{24}$$

Here s_{AN} and s_{BN} are the distances from A to N and B to N, respectively, θ is the flow inclination relative to the x axis, and the coordinate n is measured normal to x

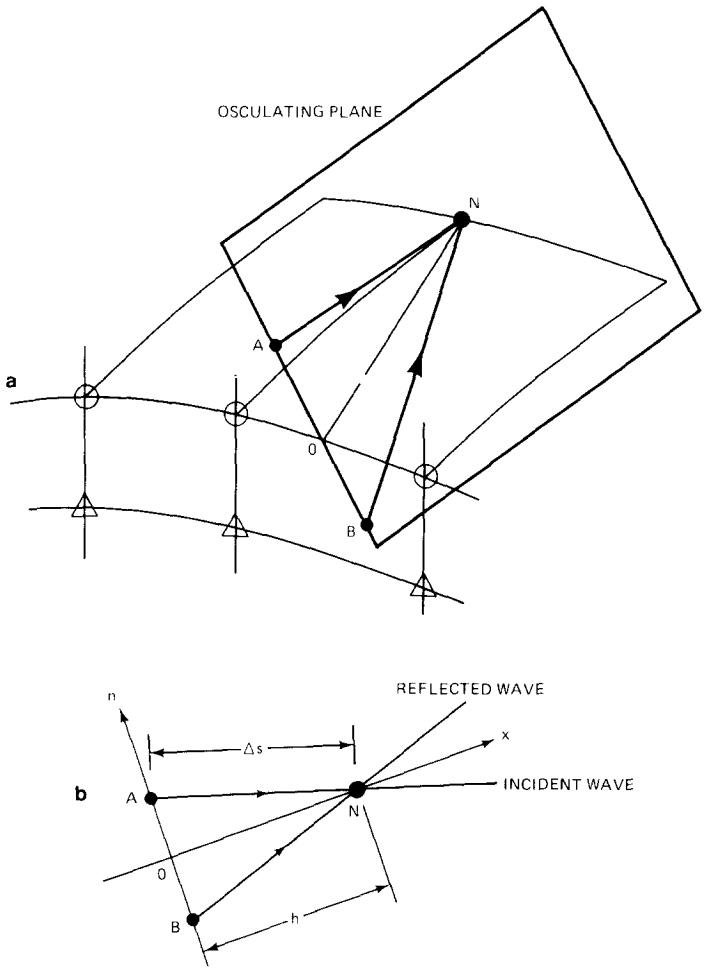

FIG. 11. Schematic showing the osculating plane for the incident and reflected waves. (a) Computational mesh. (b) Osculating plane.

(Fig. 11). By virtue of the construction of the flow properties the values at A and B are related as follows:

$$v_J = v_0 + \tfrac{1}{2}v_0'' n_J^2 + O(h^3), \tag{25}$$

$$\theta_J = \theta_0' n_J + \tfrac{1}{2}\theta_0'' n_J^2 + O(h^3), \tag{26}$$

$$K_J = K_0 + K_0' n_J + \tfrac{1}{2}K_0'' n_J^2 + O(h^3). \tag{27}$$

The subscript J can have the value A or B, $(\,)'$ denotes differentiation with respect to n, and h is the distance Δx. The values of n_A and n_B are given by

$$n_J = -h/2[\tan(\theta_J \mp \mu_J) + \tan(\theta_N \mp \mu_N)]. \tag{28}$$

Subtract Eq. (24) from Eq. (23) and solve for θ_N using Eqs. (25)–(28):

$$\theta_N = \tfrac{1}{4}K_0'(n_A - n_B)\, s_{AN} + \tfrac{1}{2}(n_A + n_B)[\theta_0' + \tfrac{1}{2}(K_B + K_N)(n_A + n_B)/(s_{BN} + s_{AN}) + \tfrac{1}{2}(v_0'' + K_0'' s_{AN})(n_A - n_B) + \tfrac{1}{2}\theta_0''(n_A^2 + n_B^2)/(n_A + n_B)] + O(h^3). \tag{29}$$

The factor $(n_A - n_B)$ and s_{AN} are both order h. Therefore, the first term in the expression for θ_N is order h^2. The factor $(n_A + n_B)$ is order $h\theta_n$ (see Appendix) and is therefore higher order.

$$\theta_N = O(h^2). \tag{30}$$

The result sought is Eq. (30). The incident/reflected wave system produced by the reflection construction produces no flow deflection to lowest order.

Conclusions

An algorithm for the boundary point calculation at a solid surface in three-dimensional flow has been proposed. It is based on an analysis of the three-dimensional wave pattern that occurs at the surface. In three-dimensional flow the body tangency condition does not uniquely determine the velocity direction at the boundary. The additional information necessary to complete the solution is contained in the wave pattern at the boundary point. For a solid surface an incident and reflected wave and a wave emitted by the body represent the interaction of the flow with the boundary. The algorithm proposed accounts for these processes in a relatively simple manner and is in fact a combination of two widely used techniques.

In the process of studying the boundary point algorithm several important concepts in three-dimensional supersonic flow were developed. Frohn [6] showed that in the osculating plane to the streamline the wave propagation is locally exactly equivalent to an axisymmetric flow. Using this concept the model problem of the infinite swept expansion or compression corner was analyzed by classical methods and by the three-dimensional osculating plane analysis. The solutions were shown to be identical. The relative orientation of the wave front to the oncoming velocity defines the binormal direction or rotation ($\hat{b}$) vector associated with the wave. The intersection of the osculating plane and the Mach cone defines the two bicharacteristics which determine the solution. At a point in a three-dimensional flow there are an arbitrary number of wave fronts each with an associated $\hat{b}$ vector. For infinitesimal strength waves a resultant $\hat{b}$ vector can be defined because infinitesimal rotations are additive.

The boundary condition at a contact surface discontinuity is the next logical problem to study. The wave analysis presented here can be used to examine that problem where there are six wave fronts at work. On each side of the contact surface an incident wave gives rise to a reflected wave and a transmitted wave on the other side of the contact surface.

APPENDIX

I. *Evaluation of* δ'

The unit vectors $\hat{q}_1$ and $\hat{q}_2$ are parallel to the initial and final velocity vectors and are related by the formula

$$\hat{q}_2 = \hat{q}_1 + \hat{R}\delta' \times \hat{q}_1, \tag{A1}$$

where $\hat{R}$ is the unit vector parallel to the rotation vector and δ' is the angular rotation between $\hat{q}_2$ and $\hat{q}_1$.

$$\hat{R} = (0, \cos\mu_n/\cos\mu, \sin\Lambda \sin\mu_n/\cos\mu).$$

Using $\hat{q}_1 = (1, 0, 0)$ in Eq. (A1),

$$\hat{q}_2 = (1, \delta' \sin\Lambda \sin\mu_n/\cos\mu, -\delta' \cos\mu_n/\cos\mu). \tag{A2}$$

Vector $\hat{q}_2$ is parallel to the surface whose normal is

$$\mathbf{n}_2 = (\delta \cos\Lambda, \delta \sin\Lambda, 1), \qquad \hat{q}_2 \cdot \mathbf{n}_2 = 0. \tag{A3}$$

Substituting Eq. (A2) in Eq. (A3) and solving for δ'

$$\delta' = \delta \cos\Lambda \cos\mu/\cos\mu_n. \tag{A4}$$

Eliminate $\cos\mu_n$ by

$$\sin\mu_n = \sin\mu/\cos\Lambda, \tag{A5}$$

$$\cos\mu_n = \sqrt{1 - \sin^2\mu_n} = \sqrt{1 - \sin^2\mu/\cos^2\Lambda} = \sqrt{\cos^2\Lambda - \sin^2\mu}/\cos\Lambda, \tag{A6}$$

$$\delta' = \delta \cos^2\Lambda \cos\mu/\sqrt{\cos^2\Lambda - \sin^2\mu}. \tag{A7}$$

II. *Derivation of Eq.* (16)

The normal vector to the cone $y^2 + z^2 = x^2 \tan^2\mu$ shown in Fig. 6b is

$$\mathbf{N} = (-\tan^2\mu, y/x, z/x). \tag{A8}$$

For the point on the cone located by the angle ξ(Fig. 6b)

$$y/x = -\tan\mu \cos\xi, \qquad z/x = \tan\mu \sin\xi.$$

Substitute into Eq. (A8) and normalize

$$\hat{n} = (-\sin\mu, -\cos\xi\cos\mu, \sin\xi\cos\mu). \tag{A9}$$

The plane tangent to the cone (and passing through the origin) is

$$-x\sin\mu - y\cos\mu\cos\xi + z\cos\mu\cos\xi = 0.$$

The trace of this plane in the $z = 0$ plane is

$$y/x = -\tan\mu/\cos\xi. \tag{A10}$$

The sweep line is given by the equation

$$y/x = -1/\tan\Lambda. \tag{A11}$$

Comparing (A10) and (A11), the value of $\cos\xi$ which corresponds to the sweep line Λ is

$$\cos\xi = \tan\mu\tan\Lambda. \tag{A12}$$

III. *Evaluation of* $\tan\xi$

Using the value of $\cos\xi$ given in Eq. (16),

$$\tan\xi = \sin\xi/\cos\xi = \sqrt{1-\cos^2\xi}/\cos\xi = \sqrt{1-\tan^2\mu\tan^2\Lambda}/\tan\mu\tan\Lambda,$$

$$\tan\xi = \sqrt{\cos^2\mu\cos^2\Lambda - \sin^2\mu\sin^2\Lambda}/\sin\mu\sin\Lambda,$$

$$\tan\xi = \sqrt{(1-\sin^2\mu)\cos^2\Lambda - \sin^2\mu(1-\cos^2\Lambda)}/\sin\mu\sin\Lambda$$

$$= \sqrt{\cos^2\Lambda - \sin^2\mu}/\sin\mu\sin\Lambda.$$

Using Eqs. (A5) and (A6),

$$\tan\xi = 1/\tan\mu_n\sin\Lambda.$$

IV *Evaluation of* $n_A + n_B$

Combine Eq. (28) (for $J = A$ and $J = B$)

$$n_A + n_B = -\tfrac{1}{2}h|\tan(\theta_A - \mu_A) + \tan(\theta_B + \mu_B) + \tan(\theta_N - \mu_N) + \tan(\theta_N + \mu_N)|.$$

Combine the tangent terms

$$n_A + n_B = -\tfrac{1}{2}h|\tan(\theta_A + \theta_B + \mu_B - \mu_A)(1 - \tan(\theta_A - \mu_A)\tan(\theta_B + \mu_B))$$
$$+ \tan 2\theta_N(1 - \tan(\theta_N - \mu_N)\tan(\theta_N + \mu_N))|.$$

Use the Taylor series expressions (such as Eq. (25)) in the first tangent term, expand this for small angles, and solve for

$$n_A + n_B = \frac{-h(\frac{1}{2}\tan 2\theta_N)[1 - \tan(\theta_N - \mu_N)\tan(\theta_N + \mu_N)]}{1 + \frac{1}{2}h\theta_0'[1 - \tan(\theta_A - \mu_A)\tan(\theta_B + \mu_B)]} = O(h^3).$$

Note. The subscript 1 has been surpressed on μ in the Appendix. Wherever μ appears without a subscript it refers to $\mu = \sin^{-1}(1/M_1)$.

REFERENCES

1. G. MORETTI, B. GROSSMAN, AND F. MARCONI, "A Complete Technique for the Calculation of Three-Dimensional Inviscid Supersonic Flows," AIAA Paper No. 72–192, 1972.
2. F. MARCONI, M. SALAS, AND L. YAEGER, "Development of a Computer Code for Calculating the Steady Super/Hypersonic Inviscid Flow Around Real Configuration, Vol. 1, Computational Technique," NASA CR-2675, April 1976.
3. S. DASH AND P. DEL GUIDICE, "Numerical Methods for the Calculation of Three Dimensional Nozzle Exhaust Flow Fields," NASA SP 347, pp. 559–702, March 1975.
4. S. RUDMAN, "Numerical Study of Highly Underexpanded Three-Dimensional Plumes," ATL TR 184, General Applied Science Labs, Westbury, N.Y., June 1973.
5. M. ABBETT, *in* "Proceedings, AIAA Computational Fluid Dynamics Conference," pp. 153–173, July 1973.
6. A. FROHN, *J. Fluid Mech.* **63** (1) (1974), 81.
7. A. FERRI, "Elements of Aerodynamics of Supersonic Flows," Macmillan Co., New York, 1949.
8. R. COURANT AND K. O. FRIEDRICKS, "Supersonic Flow and Shock Waves," Interscience, New York, 1948.
9. R. VON MISES, "Mathematical Theory of Compressible Flow," Academic Press, New York, 1958.
10. G. MORETTI AND M. ABBETT, *AIAA J.* **4** (12) (1966) 2136.
11. G. MORETTI, "The Importance of Boundary Conditions in the Numerical Treatment of Hyperbolic Equations," Polytechnic Institute of New York PIBAL Report No. 68–34, New York, November 1968.
12. T. DENEFF, "Treatment of Boundaries in Unsteady Inviscid Flow Computations," Report, LR 262, Delft University of Technology, The Netherlands, 1978.
13. S. RUDMAN, "Multinozzle Plume Flow Fields-Structure and Numerical Calculation," AIAA 10th Fluid & Plasma Dynamics Conference June 27–29," Paper No. 77–710, 1977.